Amino Acids (2013) 44:701–713
DOI 10.1007/s00726-012-1394-8

ORIGINAL ARTICLE

Covalent fusion inhibitors targeting HIV-1 gp41 deep pocket

Yu Bai · Huifang Xue · Kun Wang · Lifeng Cai · Jiayin Qiu · Shuangyu Bi · Luhua Lai · Maosheng Cheng · Shuwen Liu · Keliang Liu

Received: 13 March 2012 / Accepted: 22 August 2012 / Published online: 9 September 2012

Abstract Covalent inhibitors form covalent adducts with their target, thus permanently inhibiting a physiological process. Peptide fusion inhibitors, such as T20 (Fuzeon, enfuvirtide) and C34, interact with the N-terminal heptad repeat of human immunodeficiency virus type 1 (HIV-1) gp41 glycoprotein to form an inactive hetero six-helix bundle (6-HB) to prevent HIV-1 infection of host cells. A covalent strategy was applied to peptide fusion inhibitor design by introducing a thioester group into C34-like peptide. The modified peptide maintains the specific interaction with its target N36. After the 6-HB formation, a covalent bond between C- and N-peptides was formed by an inter-helical acyl transfer reaction, as characterized by various biophysical and biochemical methods. The covalent reaction between the reactive C-peptide fusion inhibitor and its N-peptide target is highly selective, and the reaction greatly increases the thermostability of the 6-HB. The modified peptide maintains high potency against HIV-1-mediated cell–cell fusion and infection.

Keywords HIV-1 · Gp41 · Peptide · Six-helix bundle · Covalent inhibitor

Y. Bai, H. Xue contributed equally to this work.

Electronic supplementary material The online version of this article (doi:10.1007/s00726-012-1394-8) contains supplementary material, which is available to authorized users.

Y. Bai · H. Xue · K. Wang · L. Cai · K. Liu (✉)
Beijing Institute of Pharmacology and Toxicology, 27 Taiping Road, Haidian District, Beijing 100850, China
e-mail: keliangliu55@126.com; keliangliu@yahoo.com

H. Xue · M. Cheng
Key Laboratory of Structure Based Drugs Design and Discovery of Ministry of Education, Shenyang Pharmaceutical University, Shenyang 110016, China

J. Qiu · S. Liu (✉)
School of Pharmaceutical Sciences, Southern Medical University, Guangzhou 510515, China
e-mail: liusw@smu.edu.cn

S. Bi · L. Lai
Beijing National Laboratory for Molecular Sciences, State Key Laboratory of Structural Chemistry for Unstable and Stable Species, College of Chemistry and Molecular Engineering, Peking University, Beijing 100871, China

Introduction

Human immunodeficiency virus type-1 (HIV-1) envelope glycoprotein (Env)-mediated virus–cell membrane fusion is a critical step for HIV-1 infection and in vivo propagation (Cai and Jiang 2010; Eckert and Kim 2001). HIV-1 Env is composed of surface unit gp120 and transmembrane unit gp41, which are noncovalently associated with each other, form trimer and decorate on the viral surface as spikes (Eckert and Kim 2001). HIV-1 infection is initiated by the binding of gp120 to the cellular surface receptor CD4 and a co-receptor, CCR5 or CXC4, triggering a cascade of large conformational changes of the gp120/gp41 complex from a native state to a prehairpin fusion intermediate (PHI) state and then to a fusion state. The fusion core formed at the fusion state is a six-helical bundle (6-HB), in which three gp41 N-terminal heptad repeats (NHR) form a trimeric inner core, and three C-terminal heptad repeats (CHR) pack in an antiparallel fashion against the inner NHR trimer (Chan et al. 1997). The energy released by 6-HB formation drives the apposition and subsequent fusion of viral and target cell membranes. Peptides derived from the NHR and CHR can bind to their counterparts in

gp41 to form an unproductive hetero 6-HB and prevent fusogenic 6-HB core formation, thus inhibiting HIV-1 host–cell membrane fusion and blocking viral infection (Jiang et al. 1993; Wild et al. 1992, 1994). Representative fusion inhibitors include: the first FDA-approved HIV-1 fusion inhibitor T20 (generic name: enfuvirtide; brand name: Fuzeon®) (Kilby et al. 1998; Lalezari et al. 2003), C34, T1249 (Eron et al. 2004; Lalezari et al. 2005), T2635 (Dwyer et al. 2007) and sifuvirtide (He et al. 2008b). Though highly efficient in drug-naive patients, peptide fusion inhibitors are prone to drug resistance due to the reduced binding affinities with the target in the mutated HIV-1 strains.

Covalent inhibitors have found increasing interests in drug design. (Singh et al. 2011) They act by forming irreversibly covalent adducts with their targets, thus permanently inhibiting the physiological processes (Jenkins et al. 2010; Yi et al. 2011; Jacobs et al. 2007). Covalent inhibitors interact with their targets in two steps. The first step consists of a specific binding that enables the inhibitor recognizing its target, and the second step is a followed covalent bond formation between the reaction group of the inhibitor and the specific site of the target. There is a close relationship between covalent bond formation and the molecular assembly of covalent inhibitors and their targets. The molecular assembly brings the functional groups involved into close proximity, so that the reactants are presented at high molar concentrations and in reachable positions. The assembly and folding also favors the conformational entropy and benefits the reaction thermodynamics. In the process of polypeptide biosynthesis, covalent bonds can be formed between peptides in physiological condition as a result of an inter-molecular acyl transfer reaction. (Sieber and Marahiel 2005; Fischbach and Walsh 2006) This process was recently reproduced in vitro by Ghadiri et al. who demonstrated the biomimetic catalysis of an inter-molecular acyl transfer of an amino acid ester and the bio-mimic synthesis of diketopiperazine based on a four-helical bundle structure (Leman et al. 2007; Wilcoxen et al. 2007; Huang et al. 2008).

N36/C34 6-HB has widely been used as a molecular model for studying the structure and function of HIV-1 gp41 and for fusion inhibitor design (Lu and Kim 1997; Jiang and Debnath 2000; Qi et al. 2008; Zhu et al. 2010). The X-ray crystal structure shows that three N36 (36-mer peptide derived from gp41 NHR, AA^{546} to AA^{581}, Fig. 1) form the trimerized inner core that contains three grooves and can serve as target, and three C34 (34-mer peptide derived from gp41 CHR, AA^{628} to AA^{661}, Fig. 1) bind antiparallel into the grooves as ligands. (Chan et al. 1997; Weissenhorn et al. 1997; Tan et al. 1997) The binding affinity of C-peptide fusion inhibitors with N36 and the thermostability of the 6-HB are correlated to the inhibitors' antiretroviral potency.

In this report, covalent strategy was applied to fusion inhibitor design, based on N36/C34 6-HB and an inter-helical acyl transfer reaction (Bai et al. 2012). The precise site of the C-peptide was modified with a thioester that served as an acyl donor using an orthogonal peptide synthesis strategy. The modified C-peptide retains the ability to interact specifically with N36. After 6-HB formation, a covalent bond between C- and N-peptides was then formed by an inter-helical acyl transfer reaction, as characterized by various biophysical and biochemical methods. The covalent reaction between C-peptide fusion inhibitor and its N-peptide target is highly selective, and the covalent bond greatly increases the thermostability of the 6-HB. The modified peptide retains high potency against HIV-1-mediated cell–cell fusion and infection.

Experimental section

Peptide synthesis, purification and identification

Peptides were synthesized using a CS-Bio 136 automated peptide synthesizer (CS Bio Co., Menlo Park, CA) using a standard solid-phase Fmoc chemistry protocol. All protected amino acids used were purchased from GL Biochem Ltd. (Shanghai, China). Rink amide resin (0.38–0.45 mmol/g, Nankai Hecheng S&T Co. Ltd., Tianjin, China) was used. Coupling of the amino acids (AA) was achieved using *O*-benzotriazol-1-yl-*N*,*N*,*N*′,*N*′-tetramethyl-uronium hexafluorophosphate (HBTU, GL Biochem, Shanghai, China) and diisopropylethylamine (DIEA, Acrose) as an activator and base, respectively, in *N*,*N*-dimethylformamide (DMF) solution. The Fmoc protective group was removed using 20 % piperidine/DMF. Between each coupling or Fmoc removal step, the resin was washed five times with DMF and three times with dichloromethane (DCM). The carboxy termini were, respectively, amidated upon cleavage from the resin, and the amino termini were capped with acetic acid anhydride. The peptides were cleaved from the resin and de-protected with Reagent K that contained 82.5 % trifluoroacetic acid, 5 % thioanisole, 5 % *m*-cresol, 5 % water and 2.5 % ethanedithiol. The crude products were precipitated with cold diethyl ether and lyophilized.

For peptides possessing a side chain thioester, Fmoc-L-glutamic acid *O*-allyl ester [Fmoc-Glu(OAll)-OH] was used at the thioester-modified site. After all amino acids had coupled on the resin in the peptide synthesizer, the *O*-allyl group was removed manually by 1 eq tetrakis(triphenylphosphine)palladium with 10 eq 5,5-dimethyl-1,3-cyclohexanedione as scavenger in DCM/THF (1:1) solution. Then the resin was washed five times with 0.5 % DIEA in DMF and five times with 1 M sodium diethyldithiocarbamate in DMF. 4 eq 1-Ethyl-3-(3-dimethyllaminopropyl)carbodiimide hydrochloride (EDC) and 4 eq

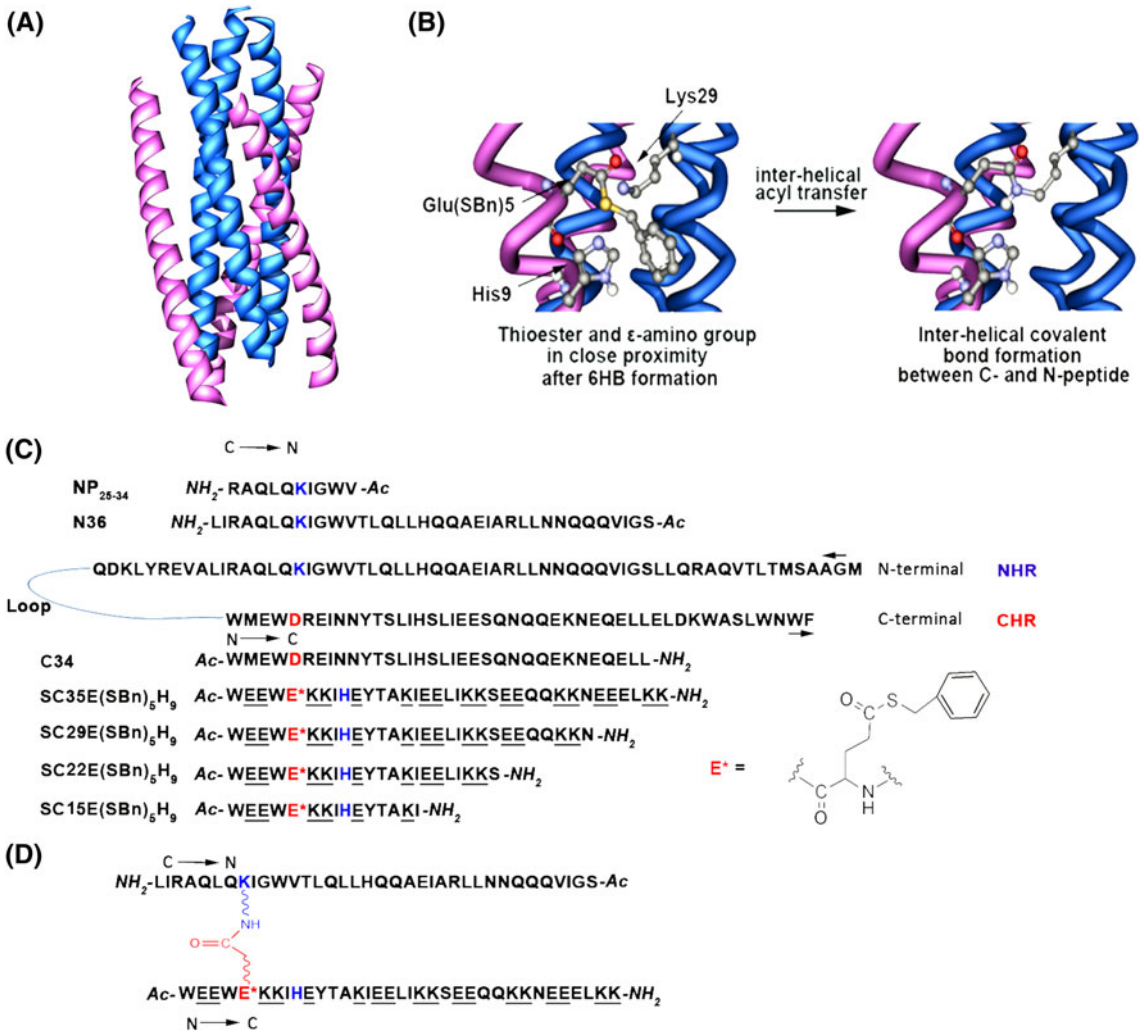

Fig. 1 Schematic representation of the HIV-1 gp41 and the N- and C-peptide sequences. **a** The structure of 6HB. **b** The site of inter-helical acyl transfer reaction. **c** Thioester-modified C-peptide sequences. **d** Covalent bond formation following the inter-helical acyl transfer reaction

benzyl mercaptan were added to the resin for thioester formation. Finally, the resin was cleaved using Reagent K.

Peptide crude products were purified by preparative reverse-phase HPLC using a Waters preparative HPLC system (PrepLC 4000): gradient elution of 30–50 % solvent B (0.1 % trifluoroacetic acid in 70 % CH_3CN/H_2O) in solvent A (0.1 % trifluoroacetic acid in H_2O) over 60 min at 16 mL/min on a Waters X-bridge C8, 10 μm, 19.5 × 250 mm column. Analytical RP-HPLC was performed on an RP-C8 column (Zorbax Eclipse XDB-C8, 5 μm, 4.6 × 150 mm) with a gradient elution of 5–100 % solvent B in solvent A over 25 min at a flow rate of 1 mL/min. Compounds were detected by UV absorption at 220 nm with a SHIMADZU SPD-10A. All peptides were purified to >95 % purity. The molecular weight of the peptides was confirmed by MALDI-TOF-MS (Autoflex III, Bruker Daltonics).

Circular dichroism (CD) spectroscopy

The N-peptides were incubated with the respective C-peptides at 37 °C for 30 min or 48 h in PBS (phosphate-buffered saline, pH 7.2). Peptides were used at a final concentration of 10 μM. The mixture was then cooled to room temperature. CD spectra were acquired at room temperature (Biologic MOS-450 4.0 nm bandwidth, 0.1 nm resolution, 0.1 cm path length, 4.0 s response time and 50 nm/min scanning speed). The spectra were corrected by subtraction of the solvent blank.

Thermal midpoint analysis was performed to determine the temperature (T_m) at which 50 % of the 6-HB would decompose. The temperature was controlled using a Biologic TCU250 system. The final concentration of N- and C-peptides was 1 μM in PBS. CD spectra were monitored at 222 nm between 20 and 90 °C (2 °C/min).

Sedimentation velocity analysis (SVA)

Sedimentation velocity measurements were performed using a Beckman XL-A analytical ultracentrifuge (Beckman Coulter, Fullerton, CA) equipped with an An60 Ti rotor and a photoelectric scanner. Two-sectored aluminum centerpieces and windows were assembled according to the manufacturer's instructions. N-peptides were incubated with C-peptides at 37 °C for 30 min in PBS (final concentration of N-peptide and C-peptide is 50 μM, respectively). The density of the sedimentation PBS buffer (0.999 g/mL) and partial specific volume [0.751 mL/g for $SC35E(SBn)_5H_9 + N36$ and $SC29E(SBn)_5H_9 + N36$, 0.757 mL/g for $SC22E(SBn)_5H_9 + N36$, and 0.755 mL/g for $SC15E(SBn)_5H_9 + N36$] were calculated using the SEDNTERP program (Laue et al. 1992). The 380 μL of the sample and 400 μL of corresponding buffer were loaded into cells. Data at 280 nm were collected at rotor speeds of 3,000 rpm initially and at 50, 000 rpm in a continuous mode with 3 min interval at 20 °C. Sedimentation coefficient distribution [$c(s)$] and molecular mass distribution [$c(M)$] were calculated from the data using the SEDFIT program (Schuck 2000).

Analysis of covalent bond formation between C- and N-peptides by tricine-SDS-polyacrylamide gel electrophoresis (tricine-SDS-PAGE)

20 % polyacrylamide gels and a BayGene Mini Cell were used for tricine-SDS-PAGE analysis. The cathode buffer was 0.1 M tricine, 0.1 M Tris and 1 % SDS, and the anode was 0.2 M Tris. N-peptide solutions were incubated with PBS at the indicated concentrations at 37 °C for 30 min before addition of C-peptides (final concentration of N- and C-peptides was 50 μM, respectively). After incubation at 37 °C for 0–48 h, the samples were mixed with Tris-SDS-glycine sample buffer (Invitrogen, Carlsbad, CA) at a ratio of 1:1 and then loaded onto the gels (20 μL/well). Gel electrophoresis was first carried out at 30 V constant voltage at room temperature for 1 h, and then at 150 V constant voltage at room temperature for 2 h. The gel was then stained with Bio-Safe Coomassie stain (Bio-Rad).

HPLC analysis of covalent bond formation between C- and N-peptides

The reactions were carried out in 1.5 mL Eppendorf tubes. A standard solution of 50 μM tryptophan (Trp) was prepared and stock solutions of N- and C-peptides were prepared by dissolving the appropriate peptides in PBS. In a typical experiment, N- and C-peptides were incubated at a 1:1 ratio at room temperature and then PBS and Trp solutions were added. The common final concentrations of the internal Trp standard, and C- and N-peptides were 25 μM. The reaction mixture was incubated at 37 °C for 0–48 h. At the indicated time, a portion of the 50 μL reaction mixture was removed and then quenched immediately with 5 μL 10 % TFA solution. Samples were frozen at −20 °C prior to HPLC analysis. Reverse-phase analytical HPLC was performed using an RP-C8 column (Agilent Zorbax Eclipse XDB-C8, 5 μm, 4.6 × 150 mm) connected to an Agilent 1200 series HPLC system with an automatic sampler. Binary solvent A and B gradients were employed at a flow rate of 1 mL/min with monitoring at 280 nm. The peptide concentrations were determined by comparison to the internal Trp standard.

Cell–cell fusion assay

The inhibitory activity of the peptides against HIV-1 env-mediated cell–cell fusion was measured as described (Wexler-Cohen and Shai 2007; Chen et al. 2011). HL2/3 cells which stably express HIV Gag, Env, Tat, Rev and Nef proteins were obtained from the AIDS Reference and Reagent Program (NIH, Dr. Barbara Felber and Dr. George Pavlakis) and used as target cells. TZM-bl cells that stably express large amounts of CD4 and CCR5 were also obtained from the AIDS Reference and Reagent Program (NIH, Dr. John C. Kappes, Dr. Xiaoyun Wu and Tranzyme Inc.). TZM-bl cells were prepared at a concentration of 5×10^5/mL (50 μL/well) in 96-well plates (Corning Costar) and incubated at 37 °C in 5 % CO_2. After a 24 h incubation, 50 μL of HL2/3 cells (2×10^6 cells/mL per well) were added to the TZM-bl cells in the presence or absence of 20 μL test inhibitors. Instead of HL2/3 cells and inhibitors, equal volumes of DMEM medium was used to establish the background signal. HL2/3 and TZM-bl cells were co-incubated for 6–8 h at 37 °C in a 5 % CO_2 atmosphere. Afterward, the medium was aspirated and the monolayer was washed carefully with PBS twice, followed by incubations with 50 μL/well of cell culture lysis reagent (Promega Corporation) for 5 min. Suspensions were then transferred to a 96-well white polystyrene plate (Corning Costar) before adding the Promega Luciferase Assay System (Promega Corporation). Fusion was measured by detecting the luciferase activity using a plate reader (Molecular Devices SpectraMax M5). Experiments were performed in duplicate and normalized to the appropriate fusion signal in the absence of inhibitors. IC_{50} values were computed by fitting a four-parameter nonlinear regression model with Origin software.

Pseudovirus assay

HIV pseudoviruses were generated as described previously (He et al. 2008a). Briefly, 293T cells (60–70 % confluent) were co-transfected with 4 μg pSF162 and 4 μg pNL4-3.luc.R-E-plasmid into six-well plate using Lipofectamin2000. The

plasmid pSF162 contains the Env of HIV-1_{SF162} strain, while pNL4-3.luc.R-E- contains an Env and Vpr defective, luciferase-expressing HIV-1 genome. Seventy-two hours after transfection, the culture supernatants were harvested and centrifuged at 2,000 rpm for 5 min. Aliquots were stored at −70 °C until use. The amount of pseudotyped particles was quantitated using the HIV-1 p24 ELISA kit (Retro-Tek, Buffalo, NY). For measuring the inhibitory activity of the test peptide against the infection of HIV pseudovirus, 100 μL U87.CCR5 cells (1×10^4/well) were seeded in 96-well plates and grown overnight. Peptide at indicated concentration was incubated with the pseudovirus (1 ng p24/well) for 30 min at 37 °C. Subsequently, the virus–peptide mixture was transferred to the cells and incubated for an additional 48 h. Cells were washed with PBS and lysed with the lysing reagent included in the luciferase kit (Promega, Madison, WI). Aliquots of cell lysates were transferred to 96-well flat bottom luminometer plates (Costar), followed by addition of luciferase substrate. The luciferase activity was measured in a microplate luminometer (Genios Pro, Tecan, US).

Results

Peptide design

The core crystal structure of the HIV-1 gp41 shows that a positively charged residue Lys574 (the 29th residue of N36, ^{29}Lys) in the pocket-forming region of the NHR (serves as target in current study) interacts with a negatively charged Asp632 (the 5th residue of C34, ^{5}Asp) residue in the pocket-binding domain of the CHR (serves as inhibitor in current study) to form an inter-helical salt bridge (Chan et al. 1997; Jiang and Debnath 2000; He et al. 2007, 2008a). Mutation experiments showed that the salt bridge played critical roles in the 6-HB stability, virus infectivity and fusion inhibitory activity (He et al. 2008a). When ^{5}Asp in the C-peptide inhibitor was mutated to a Glu, the 6-HB stability was further enhanced (He et al. 2008a). The existence of the Asp(Glu)–Lys salt bridge suggests that the side chains of these two residues are in close proximity in the 6-HB and interact specifically with each other. So, ε-amino of ^{29}Lys in N36 was selected as an acyl acceptor, and ^{5}Asp in C34 was modified to function as an acyl donor. We expected that an inter-helical covalent bond would be formed between the modified C34 inhibitor and the target after the 6-HB assembly. A His residue located at the i+4 site of the acyl donor, which has been shown to accelerate the acyl transfer reaction, was also introduced (Wilcoxen et al. 2007; Erben et al. 2011; Bai et al. 2012). To further increase the binding affinity, double salt bridges were introduced into the C34 to increase the helical interaction and the peptide's solubility (Otaka et al. 2002; Naito et al. 2009; Nishikawa et al. 2009). The resulting covalent inhibitor SC35E$(SBn)_5H_9$ (peptide **1**) contained the SC35 scaffold, its 9th site (i+4 site) was mutated to His, and the 5th residue of SC35 was mutated to Glu for modification with a side chain benzyl thioester. Shorter covalent fusion inhibitors were also designed for structure–activity relationship study, resulting in 29-mer, 22-mer and 15-mer peptide covalent inhibitors. Unmodified peptides with the same sequences were also synthesized as controls. The designed peptide sequences are presented in Fig. 1.

Thioester-modified C-peptides interact with N36 to form 6-HB complex

The modified peptides should retain the ability to selectively recognize their target to be efficient covalent inhibitors. We first characterized the secondary structure of the modified C-peptide thioester and its interaction with the N36 target using CD spectroscopy, and compared the results with those of the unmodified peptide. In general, C-peptide fusion inhibitors are partially α-helical in solution, while 6-HBs are characterized as nearly full α-helix in CD spectra. The higher helicities of C-peptides are considered correlating to tighter binding with their NHR target (Otaka et al. 2002). SC35E$(SBn)_5H_9$ formed a typical α-helical structure as evidenced by the double minima at 208 and 222 nm in CD spectra. The α-helical content is 81 % based on the $[\theta]_{222nm}$ value (Liu et al. 2010; Bai et al. 2011), which is significantly higher than that of unmodified $SC35E_5H_9$ (33 % α-helix) (Fig. 2; Table 1). SC35E$(SBn)_5H_9$ formed a typical 6-HB structure with 99 % α-helicity when co-incubated with N36, whereas the control complex, $SC35E_5H_9$/N36, showed 87 % α-helicity. The shorter peptides, SC29E$(SBn)_5H_9$, $SC29E_5H_9$, SC22E$(SBn)_5H_9$ and $SC22E_5H_9$ also formed 6HB structures with N36. However, when SC15E$(SBn)_5H_9$ or $SC15E_5H_9$ was mixed with N36, no complex of high-helical structure was observed due to their limited sites available for interactions with N36. Thermodenaturation analysis showed similar T_m for SC35E$(SBn)_5H_9$/N36 (72 °C) as those of $SC35E_5H_9$/N36 (76 °C). These results suggested that the thioester-modified SC35E$(SBn)_5H_9$ retained the ability to interact with N36 to form the 6-HB structure.

The 6-HBs were further characterized by sedimentation velocity analysis (SVA). SVA provides hydrodynamic information regarding the size and shape of different macromolecules. It is particularly useful for quantitatively charactering self- or hetero-association behaviors of biomolecules in solution. When SC35E$(SBn)_5H_9$ was mixed with N36 at an equal molar ratio in PBS, the major species showed a sedimentation coefficient of 2.402 s, corresponding to a molecular mass of 26,439 Da, consistent with

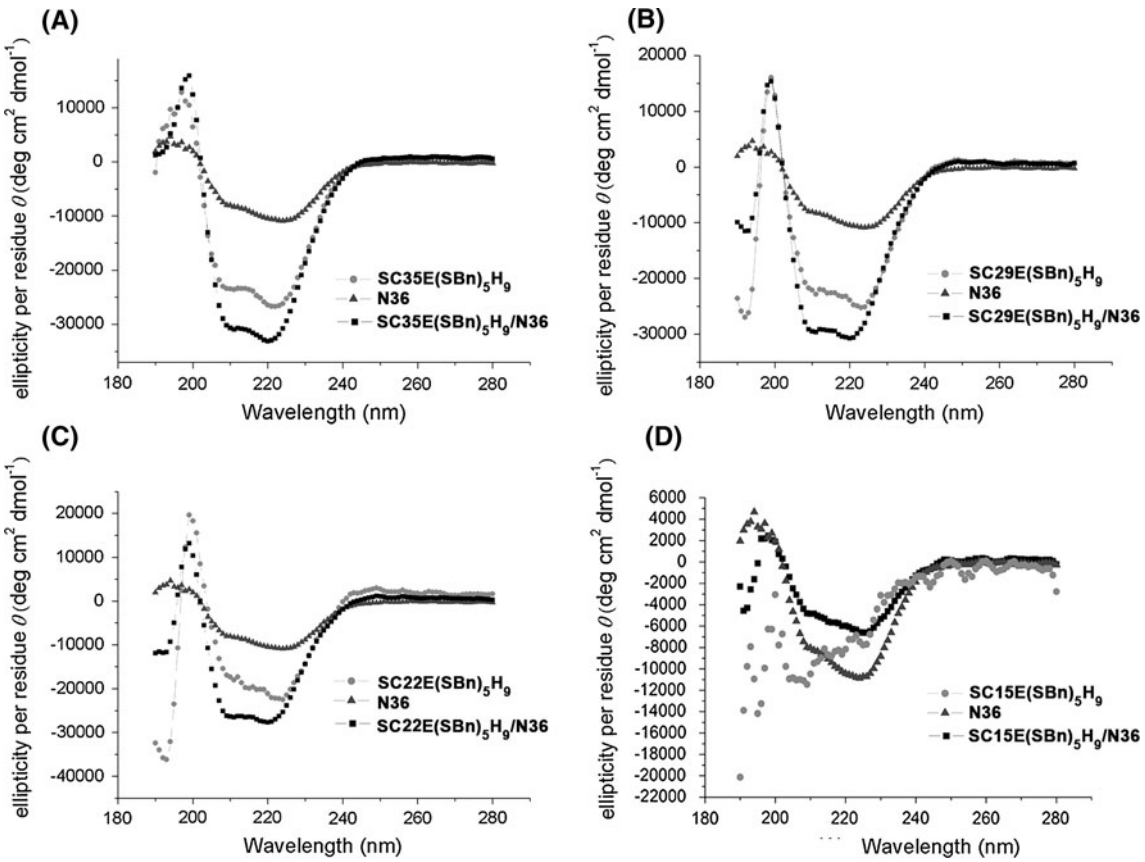

Fig. 2 CD spectra of peptides and their respective complexes. **a** $SC35E(SBn)_5H_9$+N36. **b** $SC29E(SBn)_5H_9$+N36. **c** $SC22E(SBn)_5H_9$+N36. **d** $SC15E(SBn)_5H_9$ + N36

the calculated molecular weight of $SC35E(SBn)_5H_9$/N36 6-HB (Fig. 3; Table 2). Combined with CD results, these observations verified that $SC35E(SBn)_5H_9$ associated with the N36 to form the typical 6-HB structure. The short peptide $SC29E(SBn)_5H_9$ or $SC22E(SBn)_5H_9$ can also form 6-HB structure with N36. However, the shortest peptide $SC15E(SBn)_5H_9$ could not form 6-HB with N36, as evidenced by CD and SVA analysis (Fig. 2; Tables 1, 2).

$SC35E(SBn)_5H_9$ forms covalent adducts with N-peptides after 6-HB formation through an inter-helical acyl transfer reaction

The capability of $SC35E(SBn)_5H_9$ to form the 6-HB with N36 suggested that the thioester-modified C-peptide retained the ability to recognize the N-peptide target. The 6-HB assembly may enable the acyl donor in the C-peptide (thioester group) accessible to the acyl acceptor in the N-peptide (^{29}Lys). We first studied the inter-chain acyl transfer by tricine-SDS polyacrylamide gel electrophoresis (tricine-SDS-PAGE). $SC35E(SBn)_5H_9$ was incubated with N36 at equimolar concentrations at 37 °C. Samples were taken from the reaction mixture at different times and stored in −20 °C for PAGE analysis. As shown in Fig. 4, the 6-HB formed by $SC35E(SBn)_5H_9$ and N36 was almost completely dissociated in the presence of SDS, as evidenced by two peptide bands identified for isolated N36 and $SC35E(SBn)_5H_9$, respectively in the SDS-PAGE at 0 h, suggesting no covalent bond formed between N36 and $SC35E(SBn)_5H_9$. As the reaction advanced, a new band with higher molecular weight appeared, indicating that a new product was generated in the reaction mixture. The reaction was almost complete in 72 h, and no N36 and $SC35E(SBn)_5H_9$ band was observed in the gel.

The inter-helical acyl transfer reaction was further confirmed by RP-HPLC. The reaction mixture contained 25 μM of N36 and C-peptides. After 5 min of incubation at 37 °C, the main products in the mixture were $SC35E(SBn)_5H_9$ and N36 and were shown as peaks *b* and *c* in Fig. 5a. The reaction was almost complete (>90 %) after 48 h of incubation at 37 °C, both N36 and $SC35E(SBn)_5H_9$ peaks almost disappeared, and a new peak with an elution time of 12.87 min (peak *d*) dominated the reaction mixture, corresponding to covalently linked N36 and $SC35E(SBn)_5H_9$. The molecular weight of the new product was determined to be 8642.6 Da by MALDI-TOF-MS (Fig. 5b), consistent with the anticipated molecular

Table 1 CD spectroscopy data of modified C-peptides, N-peptide and their complexes

Peptides	θ_{222nm}	α-helix (%)	T_m (°C)	T_m after 48 h (°C)[a]
N36	−10,655	32	N.D	N.D
$SC35E(SBn)_5H_9$	−26,686	81	N.D	N.D
$SC35E_5H_9$	−10,745	33	N.D	N.D
$SC29E(SBn)_5H_9$	−24,902	76	N.D	N.D
$SC29E_5H_9$	−4,127	13	N.D	N.D
$SC22E(SBn)_5H_9$	−22,181	67	N.D	N.D
$SC22E_5H_9$	−4,577	14	N.D	N.D
$SC15E(SBn)_5H_9$	−7,245	22	N.D	N.D
$SC15E_5H_9$	−829	3	N.D	N.D
C34+N36 Bai et al. (2011)	−27,060	82	57	N.D
$SC35E(SBn)_5H_9$+N36	−32,577	99	72	>90
$SC35E_5H_9$+N36	−28,735	87	76	75
$SC29E(SBn)_5H_9$+N36	−29,897	91	52	>90
$SC29E_5H_9$+N36	−22,665	69	50	47
$SC22E(SBn)_5H_9$+N36	−27,023	82	43	>90
$SC22E_5H_9$ + N36	−25,445	77	44	42
$SC15E(SBn)_5H_9$+N36	−6,274	19	N.D	N.D
$SC15E_5H_9$+N36	−6,915	21	N.D	N.D
NP_{25-34}	−1,320	4	N.D	N.D
$SC35E(SBn)_5H_9$+NP_{25-34}	−20,875	63	N.D	N.D

ND not determined

[a] The Tm of 6-HB was determined after 48 h of incubation at 37 °C

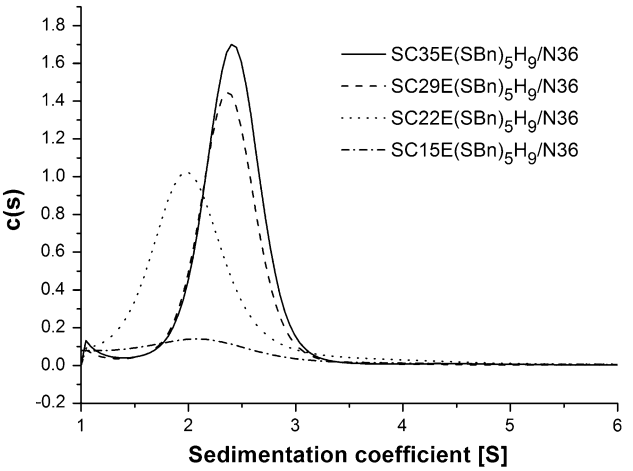

Fig. 3 Sedimentation velocity analysis of thioester-modified C-peptides and N36 complexes

Table 2 Thioester-modified C-peptides and N36 complex SVA results

Peptides	Sedimentation coefficient (S)	Observed MW (Da)	Calculated 6-HB MW (Da)
$SC35E(SBn)_5H_9$+N36	2.402	26,439	26,313
$SC29E(SBn)_5H_9$+N36	2.406	24,632	24,048
$SC22E(SBn)_5H_9$+N36	2.119	20,259	21,390
$SC15E(SBn)_5H_9$+N36	N.D[a]	N.D	18,903

[a] The data could not be detected

weight of the acyl transfer product, suggesting that a covalent bond formed between ε-amino of ^{29}Lys in N36 and ^{5}Glu in $SC35E(SBn)_5H_9$ as expected. The peak *e* in HPLC (Fig. 5a) was identified as $SC35E_5H_9$ by HPLC and MALDI-TOF MS (data not shown), suggesting that during the incubation, a small amount of thioester on $SC35E(SBn)_5H_9$ hydrolyzed spontaneously.

To investigate the relationship between the 6-HB assembly and the inter-helical acyl transfer reaction, different lengths of covalent C-peptide inhibitors were tested. $SC29E(SBn)_5H_9$ and $SC22E(SBn)_5H_9$, which formed 6-HB with N36, formed inter-helix covalent bond with N36. $SC15E(SBn)_5H_9$ that could not form 6-HB with N36 did not react with N36 under the same conditions. These results suggested that a specific association between the modified C-peptide inhibitors and the NHR target was required for inter-helical covalent bond formation. To facilitate the acyl transfer reaction, the acyl donor must be in close proximity to the acyl acceptor in the assembly. RP-HPLC was used to determine the reaction rate, and the reaction rates of C-peptide with different lengths are summarized in Table 3. Interestingly, the shortest 6-HB forming peptide

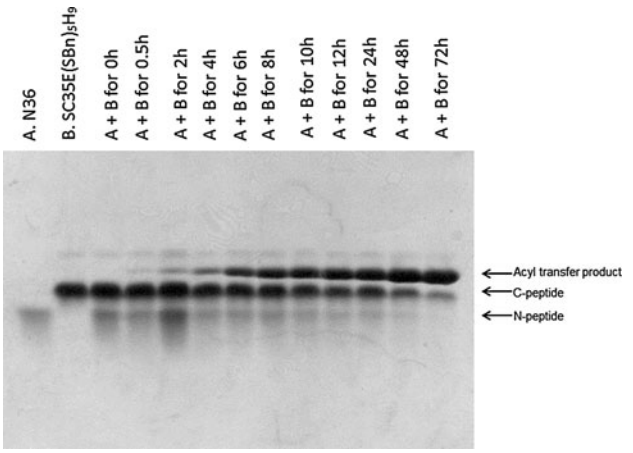

Fig. 4 SDS-tricine-PAGE analysis of $SC35E(SBn)_5H_9$ and N36. *Lane 1*, N36; *lane 2*, $SC35E(SBn)_5H_9$ and *lanes* 3–13, $SC35E(SBn)_5H_9$ incubated with N36 at an equal molar ratio in PBS at 37 °C for 0, 0.5, 2, 4, 6, 8, 10, 12, 24, 48 and 72 h, respectively

$SC22E(SBn)_5H_9$ had the highest reaction rate, while the longest peptide $SC35E(SBn)_5H_9$ had the lowest reaction rate, in contrast to their 6-HB thermostability. This suggested

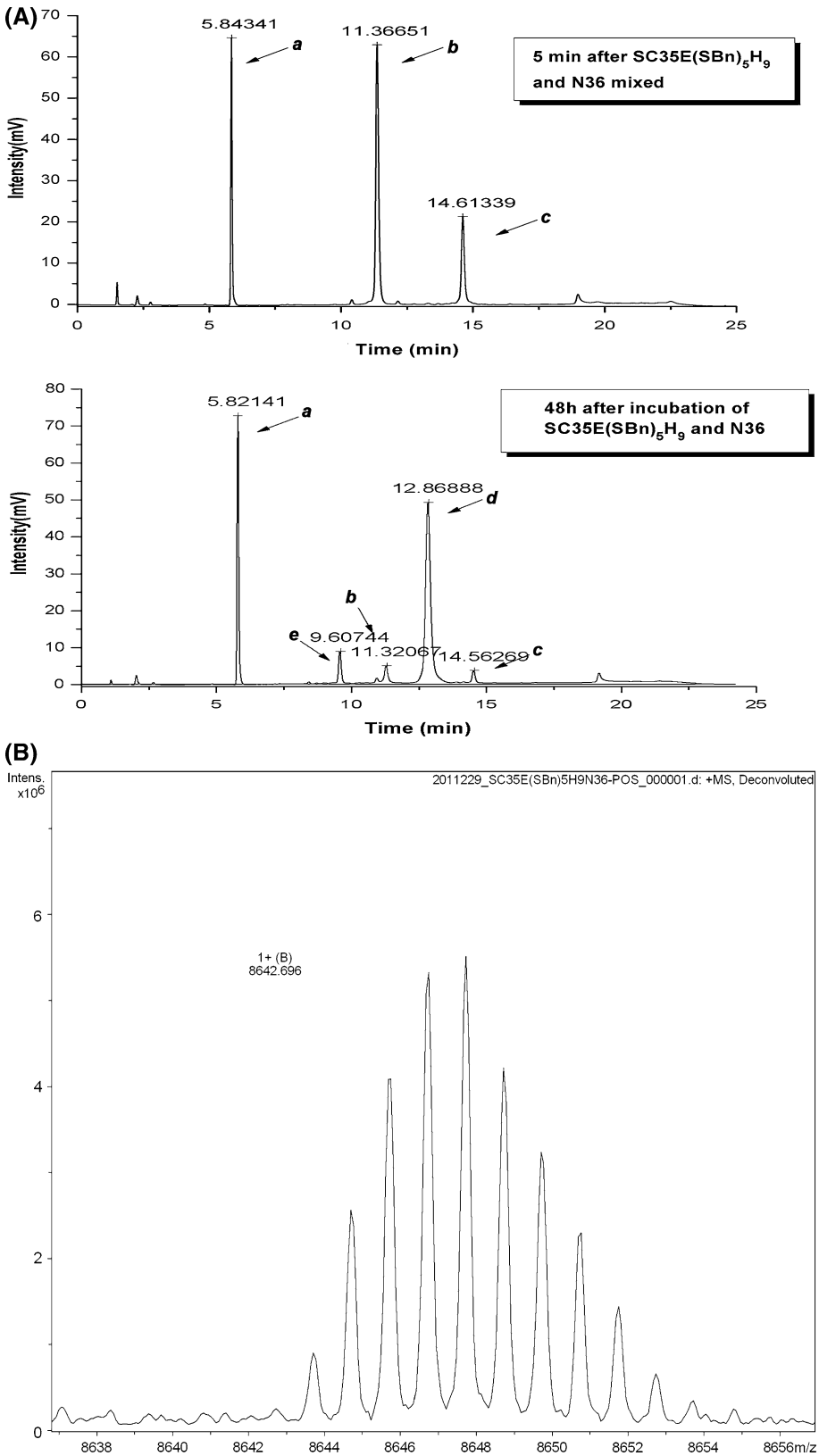

Fig. 5 The HPLC (**a**) and MALDI-TOF-MS (**b**) analysis of the acyl transfer reaction. In HPLC (**a**), *a* Trp; *b* $SC35E(SBn)_5H_9$; *c* N36, *d* the acyl transfer product; *e* the thioester hydrolysis product of C-peptide. The reaction mixture contained 25 μM of N36 and $SC35E(SBn)_5H_9$ at 37 °C

that as long as the 6-HB assembly occurred, the acyl donor and acceptor were close enough to facilitate acyl transfer. The slight difference in reaction rates among C-peptide covalent inhibitors with different lengths may be due to the effect of the assembly to the energy barrier in the reaction transition state, which may need further investigation.

Table 3 The rate constant and $t_{1/2}$ of the inter-helical acyl transfer reaction

Peptides	k_2 (M^{-1} s^{-1})	$t_{1/2}$ (h)
$SC35E(SBn)_5H_9$	1.32	8.4
$SC29E(SBn)_5H_9$	2.57	4.3
$SC22E(SBn)_5H_9$	4.81	2.5

The inter-helical acyl transfer reaction could only occur after the 6HB formation

A covalent inhibitor should only react with its target rather than reacting intra-molecularly or with other irrelevant biomolecules. Therefore, reactivity and specificity are both crucial for a covalent inhibitor. $NP_{25\text{-}34}$, a 10-mer segment of N36 containing ^{29}Lys, is too short to form 6-HB with $SC35E(SBn)_5H_9$ (Table 1), and it did not react with the thioester-modified C-peptides even after 48 h of incubation at 37 °C (Fig. 6). It is worth noting that though there are nine Lys residues in $SC35E(SBn)_5H_9$, when it was incubated with $NP_{25\text{-}34}$ or incubated alone in PBS for 48 h, no new product such as cyclic peptide or dimeric peptide was detected. These results suggested that the reaction between free amino and free thioester was too slow to be detected under the experimental conditions. It also indicated that the inter-helical acyl transfer reaction between $SC35E(SBn)_5H_9$ and N36 proceeded in two steps: a molecular assembly and an acyl transfer. Only when 6-HB formation occurred and the acyl donor on C-peptide and the acyl acceptor on N-peptide were assembled into precise sites in close proximity, the acyl transfer reaction could occur. Therefore, $SC35E(SBn)_5H_9$ is a covalent inhibitor specifically targeting the NHR region of the HIV-1 gp41.

Covalent bond formation greatly increases the thermostability of 6-HB

Structure–activity relationship studies of HIV-1 peptide fusion inhibitors showed that the inhibitory activities of fusion inhibitors were correlated to 6-HB stability. The thermostabilities of 6-HBs formed by covalent fusion inhibitors were studied by thermal denaturing and monitoring the secondary structure change by CD signal at 222 nm. As shown in Fig. 7, before covalent bond formation, $SC35E(SBn)_5H_9$/N36 showed a typical two-state thermal transition with T_m value of 72 °C. After inter-helical covalent bond formation, no obvious thermal denaturing was observed even at 90 °C, the highest temperature tested for the instrument. This is consistent with other observations (Zhou et al. 1993; Bianchi et al. 2005) when a covalent bond was introduced into the coiled-coil structure, suggesting that covalent interaction between the C-peptide fusion inhibitor and the NHR target greatly increased the stability of the adducts formed.

Covalent peptide fusion inhibitors exhibit high potency against HIV-mediated cell–cell fusion and HIV infection

The activities of the covalent fusion inhibitors against the HIV-1-cell membrane fusion were accessed using an HIV-

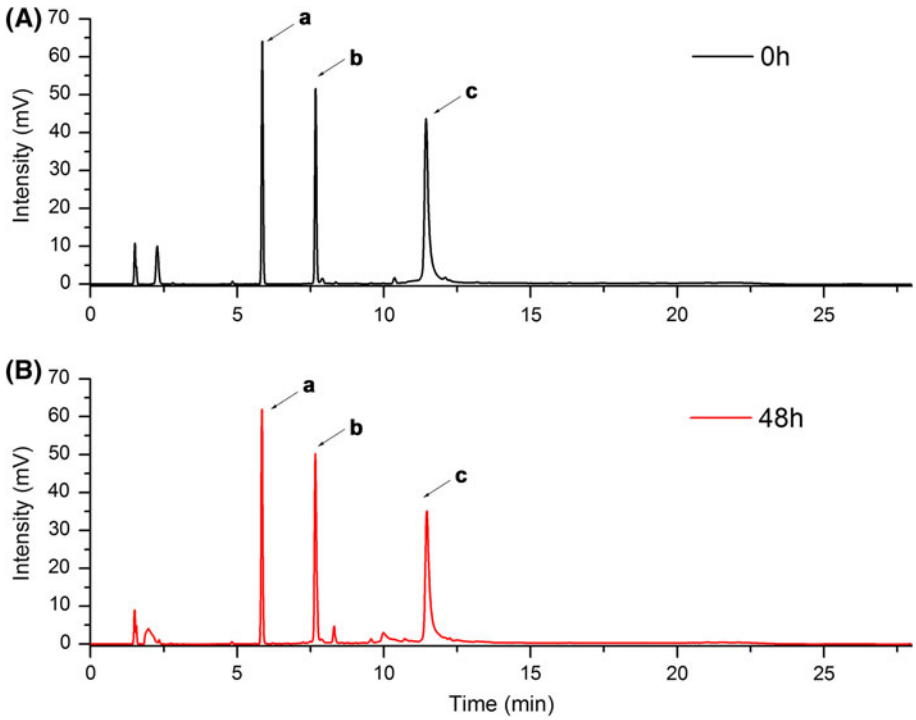

Fig. 6 The HPLC analysis of $SC35E(SBn)_5H_9$ and $NP_{25\text{-}34}$ for 0 h (**a**) and 48 h (**b**) co-incubation at 37 °C. *a* Interior standard Trp, *b* $NP_{25\text{-}34}$, *c* $SC35E(SBn)_5H_9$

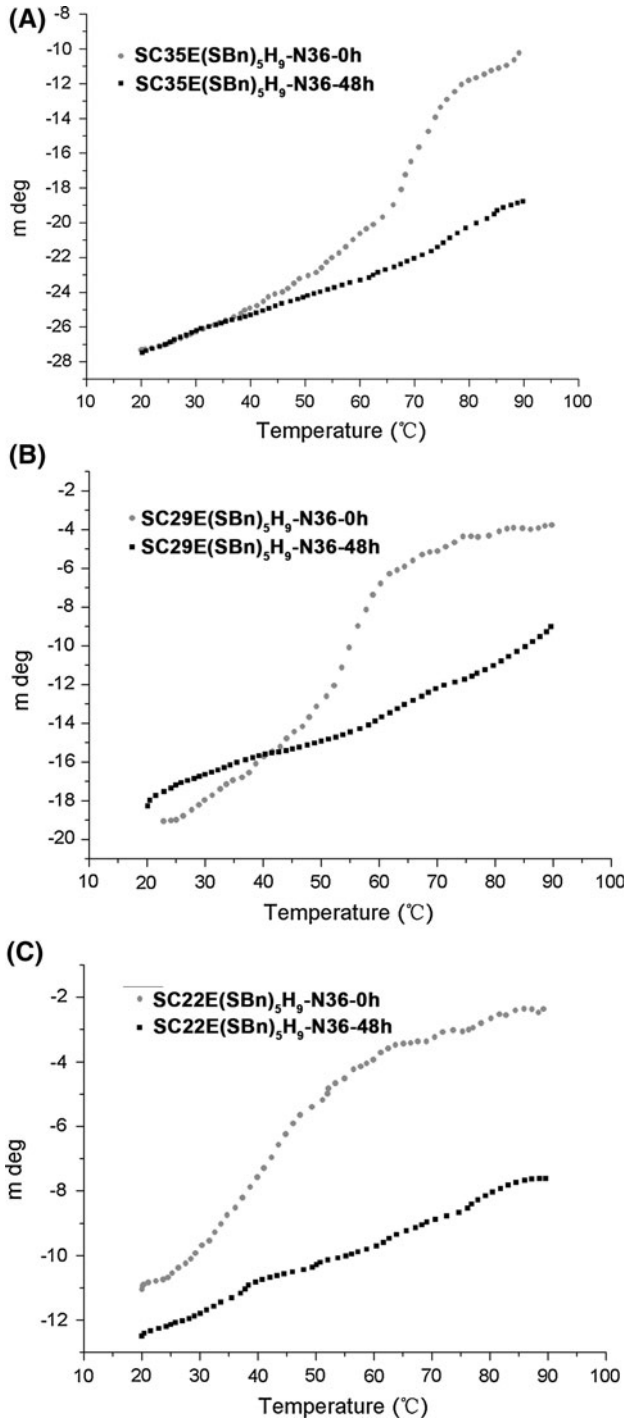

Fig. 7 The thermal denaturation curves of 6HBs with or without inter-helical covalent bond. Ellipticities at 222 nm from 20 to 90 °C (2 °C/min) were used to determine T_m. The peptides were 1 μM in PBS (pH 7.2), and the C- and N-peptide were in equimolar concentrations. **a** $SC35E(SBn)_5H_9$+N36. **b** $SC29E(SBn)_5H_9$+N36. **c** $SC22E(SBn)_5H_9$+N36

1-mediated cell–cell fusion assay. The inhibitor concentration that elicited 50 % inhibition (IC_{50}) was 1.02 ± 0.33 nM for $SC35E(SBn)_5H_9$, similar to the unmodified peptide $SC35E_5H_9$ (2.24 ± 0.78 nM) and C34 (1.59 ± 0.10 nM). Other thioester-modified peptides also showed similar IC_{50} values compared to their unmodified peptide counterparts (Table 4).

Table 4 Anti-fusogenic activity assessment using cell–cell fusion and pseudovirus assays

Peptides	IC_{50} (nM, cell–cell fusion)	IC_{50} (nM, pseudovirus)
C34	1.59 ± 0.10	4.24 ± 1.31
$SC35E(SBn)_5H_9$	1.02 ± 0.33	3.50 ± 0.50
$SC35E_5H_9$	2.24 ± 0.78	4.33 ± 0.65
$SC29E(SBn)_5H_9$	5.79 ± 1.27	14.46 ± 8.10
$SC29E_5H_9$	4.68 ± 1.18	4.27 ± 1.39
$SC22E(SBn)_5H_9$	928 ± 144	>1,000
$SC22E_5H_9$	1,290 ± 130	>1,000
$SC15E(SBn)_5H_9$	27,800 ± 9,790	>1,000
$SC15E_5H_9$	62,200 ± 14,300	>1,000

We then tested the anti-HIV-1 activities of the covalent fusion inhibitors using a pseudovirus assay. Consistent with cell–cell fusion assay, the covalent fusion inhibitors showed similar activities against HIV-1 infection in the pseudovirus assay (Table 4). Combined with cell–cell fusion assay results, we concluded that the covalent fusion inhibitors retained the ability to interact with gp41 target and inhibit HIV-1 infection.

Discussion and conclusions

In antiretroviral therapy, drug resistance is the main issue and drug-resistant HIV-1 isolates can emerge rapidly, usually as early as in clinical trials. For HIV-1 fusion inhibitors, the target gp41 NHR, though highly conserved among HIV-1 isolates in drug-naive patients, undergoes fast mutation when treated with fusion inhibitors. These mutations weaken the interaction between fusion inhibitors and the gp41 NHR target. Covalent inhibitors may provide an alternative for peptide fusion inhibitor design to overcome the weak binding between the fusion inhibitor and target associated with drug-resistant mutations.

The designed covalent HIV-1 fusion inhibitor $SC35E(SBn)_5H_9$ fulfills two criteria for a covalent inhibitor: it retains the ability to specifically interact with its target, and it can form a covalent bond to link the target thereafter. For a covalent inhibitor, the activity of the reaction groups plays a dual and controversial role. Basically, it should be active enough to facilitate the covalent formation after recognizing the target; on the other hand, reaction groups that are too active hold the potential of nonspecific reaction with unrelated sites. The covalent

bond is readily formed between designed covalent inhibitors of different lengths as long as the peptide can specifically interact with the gp41 NHR target. The covalent formation is highly selective since a short peptide contains the same thioester group, but it is too short to recognize its target. Therefore, the short thioester-modified peptide will not form a covalent bond with the NHR target. SC35E$(SBn)_5H_9$ also could not react with unassembled peptides in spite of Lys residues inside.

Covalent fusion inhibitors retain their activity in HIV-1 gp41-mediated cell–cell fusion assay and infection assays using HIV-1 psudoviruses. Other reported covalent HIV-1 fusion inhibitors, such as maleimide modified C34 (Jacobs et al. 2007; Yi et al. 2011), showed similar antiviral activity with C34. Those maleimide modified C34 can form a covalent bond with gp41 and permanently attach the viral membrane, as evidenced by a temperature-arrested state (TAS) prime-wash assay. However, the authors mutated the ^{28}Lys on the maleimide modified C34 to prevent the reaction between the maleimide and the ^{28}Lys on C-peptide implying that there may be a problem of selectivity for maleimide to amino groups. SC35E$(SBn)_5H_9$, with similar interacting mechanism, should act by permanently attaching to gp41 NHR target and irreversibly inhibit HIV-1 infection. The high activity of SC35E$(SBn)_5H_9$ suggests its potential application in antiretroviral therapy; the detailed mechanism studies of its interaction with the gp41 NHR target may justify this class of covalent fusion inhibitors used as tools to study the mechanism of HIV-1 gp41-mediated virus–cell membrane fusion for new fusion inhibitor design.

In conclusion, covalent fusion inhibitors were designed based on a well-studied C-peptide inhibitor, C34, by introducing thioester as the reactive group. These covalent fusion inhibitors retain the ability to recognize their target HIV-1 gp41 NHR. After proper assembly, an inter-helical covalent bond is formed between the inhibitors and their target via an acyl transfer reaction. These covalent fusion inhibitors also retain high potency against HIV-1 gp41-mediated cell–cell fusion and replication. The covalent bond formed between the inhibitor and target may make the inhibitor permanently attach to the target and irreversibly inhibit the HIV-1 gp41 function, and thus have potential to maintain high activity against drug-resistant HIV-1 isolates. However, there were no obvious improvements of the modified peptides in their IC50 in cell–cell fusion and pseudovirus assays with their corresponding unmodified peptides. The velocity of inter-helical acyl transfer reaction should be enhanced in future studies for designing covalent inhibitors with higher potency.

Acknowledgments This work was support by the Natural Science Foundation of China Grants (No. 81072581 and No. U0832001) and Key Tech. of National S&T Major Project of Original New Drug Research grant (2012ZX09301-003-001).

Conflict of interest All the authors declare that they have no conflict of interest.

References

Bai Y, Ling Y, Shi W, Cai L, Jia Q, Jiang S, Liu K (2011) Heteromeric assembled polypeptidic artificial hydrolases with a six-helical bundle scaffold. ChemBioChem 12:2647–2658

Bai Y, Xue H, Ling Y, Cai L, Cheng M, Liu K (2012) Inter-chain acyl transfer reaction in a peptide six-helical bundle: a model for regulating the interaction between peptides or proteins by a chemical method. Chem Commun 48:4320–4322

Bianchi E, Finotto M, Ingallinella P, Hrin R, Carella AV, Hou XS, Schleif WA, Miller MD, Geleziunas R, Pessi A (2005) Covalent stabilization of coiled coils of the HIV gp41 N region yields extremely potent and broad inhibitors of viral infection. Proc Nat Acad Sci USA 102(36):12903–12908. doi:10.1073/pnas.0502449102

Cai L, Jiang S (2010) Development of peptide and small-molecule HIV-1 fusion inhibitors that target gp41. ChemMedChem 5(11):1813–1824. doi:10.1002/cmdc.201000289

Chan DC, Fass D, Berger JM, Kim PS (1997) Core structure of gp41 from the HIV envelope glycoprotein. Cell 89(2):263–273

Chen W, Xu L, Cai L, Zheng B, Wang K, He J, Liu K (2011) d(TGGGAG) with 50-nucleobase-attached large hydrophobic groups as potent inhibitors for HIV-1 envelop proteins mediated cell–cell fusion. Bioorg Med Chem Lett 21:5762–5764

Dwyer JJ, Wilson KL, Davison DK, Freel SA, Seedorff JE, Wring SA, Tvermoes NA, Matthews TJ, Greenberg ML, Delmedico MK (2007) Design of helical, oligomeric HIV-1 fusion inhibitor peptides with potent activity against enfuvirtide-resistant virus. Proc Nat Acad Sci USA 104(31):12772–12777. doi:10.1073/pnas.0701478104

Eckert DM, Kim PS (2001) Mechanisms of viral membrane fusion and its inhibition. Annu Rev Biochem 70:777–810

Erben A, Grossmann TN, Seitz O (2011) DNA-triggered synthesis and bioactivity of proapoptotic peptides. Angew Chem Int Edn 50(12):2828–2832. doi:10.1002/anie.201007103

Eron JJ, Gulick RM, Bartlett JA, Merigan T, Arduino R, Kilby JM, Yangco B, Diers A, Drobnes C, DeMasi R, Greenberg M, Melby T, Raskino C, Rusnak P, Zhang Y, Spence R, Miralles GD (2004) Short-term safety and antiretroviral activity of T-1249, a second-generation fusion inhibitor of HIV. J Infect Dis 189(6):1075–1083. doi:10.1086/381707

Fischbach MA, Walsh CT (2006) Assembly-line enzymology for polyketide and nonribosomal peptide antibiotics: logic, machinery, and mechanisms. Chem Rev 106(8):3468–3496. doi:10.1021/cr0503097

He Y, Liu S, Jing W, Lu H, Cai D, Chin DJ, Debnath AK, Kirchhoff F, Jiang S (2007) Conserved residue Lys574 in the cavity of HIV-1 Gp41 coiled-coil domain is critical for six-helix bundle stability and virus entry. J Biol Chem 282(35):25631–25639

He YX, Liu SW, Li JJ, Lu H, Qi Z, Liu ZH, Debnath AK, Jiang SB (2008a) Conserved salt bridge between the N- and C-terminal heptad repeat regions of the human immunodeficiency virus type 1 gp41 core structure is critical for virus entry and inhibition. J Virol 82(22):11129–11139. doi:10.1128/jvi.01060-08

He YX, Xiao YH, Song HF, Liang Q, Ju D, Chen X, Lu H, Jing WG, Jiang SB, Zhang LQ (2008b) Design and evaluation of sifuvirtide, a novel HIV-1 fusion inhibitor. J Biol Chem 283(17):11126–11134. doi:10.1074/jbc.M800200200

Huang ZZ, Leman LJ, Ghadiri MR (2008) Biomimetic catalysis of diketopiperazine and dipeptide syntheses. Angew Chem Int Edn 47(9):1758–1761. doi:10.1002/anie.200704266

Jacobs A, Quraishi O, Huang XC, Bousquet-Gagnon N, Nault G, Francella N, Alvord WG, Pham N, Soucy C, Robitaille M, Bridon D, Blumenthal R (2007) A covalent inhibitor targeting an intermediate conformation of the fusogenic subunit of the HIV-1 envelope complex. J Biol Chem 282(44):32406–32413. doi:10.1074/jbc.M705577200

Jenkins LMM, Ott DE, Hayashi R, Coren LV, Wang DY, Xu Q, Schito ML, Inman JK, Appella DH, Appella E (2010) Small-molecule inactivation of HIV-1 NCp7 by repetitive intracellular acyl transfer. Nat Chem Biol 6(12):887–889. doi:10.1038/nchembio.456

Jiang S, Debnath AK (2000) A salt bridge between an N-terminal coiled coil of gp41 and an antiviral agent targeted to the gp41 core is important for Anti-HIV-1 activity. Biochem Biophys Res Commun 270(1):153–157

Jiang SB, Lin K, Strick N, Neurath AR (1993) HIV-1 inhibition by a peptide. Nature 365(6442):113–113

Kilby JM, Hopkins S, Venetta TM, DiMassimo B, Cloud GA, Lee JY, Alldredge L, Hunter E, Lambert D, Bolognesi D, Mathews T, Johnson MR, Nowak MA, Shaw GM, Saag MS (1998) Potent suppression of HIV-1 replication in humans by T-20, a peptide inhibitor of gp41-mediated virus entry. Nat Med 4(11):1302–1307

Lalezari JP, Henry K, O'Hearn M, Montaner JSG, Piliero PJ, Trottier B, Walmsley S, Cohen C, Kuritzkes DR, Eron JJ, Chung J, DeMasi R, Donatacci L, Drobnes C, Delehanty J, Salgo M, Farthing C, Graham E, Packard M, Ngo L, Lederman M, Buam J, Pollard R, Rauf S, Silkowski W, Thompson M, Rucker A, Harris M, Larsen G, Preseon S, Cunningham D, Guimaraes D, Bertasso A, Kinchelow T, Myers R, Phoenix B, Skolnik PR, Adams B, Leite OHM, Oliveira M, Lefebvre E, Gomez B, Foy KB, Lampiris H, Charles S, Dobkin J, Crawford M, Slom T, Murphy R, Mikaitis T, Witek J, Anthony R, Richmond G, Appleby VF, Smaill F, Kelleher L, Nieto L, Trevino S, Schechter M, Fonseca B, DeJesus E, Ortiz R, Wheat J, Goldman M, O'Connor DK, Sierra-Madero JG, Nino-Oberto S, Gallant JE, Apuzzo L, Basgoz N, Habeeb K, Alpert P, Thomas S, Miller T, Kempner T, Wolfe PR, Bautista J, Martin HL, Morton ME, Henry D, Kilcoyne S, Glutzer E, Rivera-Vazquez C, Pomales Z, Bellos N, Hoffman LA, Olmscheid B, Klein O, Miller M, Steinhart CR, Liebmann A, Williams S, Springate L, Logue K, Smiley L, Miralles GD, Haubrich R, Nuffer K, Beatty G, O'Leary S, Rouleau D, Dufresne S, Kilby JM, Saag M, Upton K, Feinberg J, Kohler P, Campbell TB, Putnam BA, Riddler SA, Rosener RR, Barnett BJ, Hansen I, Collier AC, Royer BA, Haas DW, Morgan M, Sathasivam K, Hersch J, Grp TS (2003) Enfuvirtide, an HIV-1 fusion inhibitor, for drug-resistant HIV infection in North and South America. N Engl J Med 348(22):2175–2185

Lalezari JP, Bellos NC, Sathasivam K, Richmond GJ, Cohen CJ, Myers RA, Henry DH, Raskino C, Melby T, Murchison H, Zhang Y, Spence R, Greenberg ML, DeMasi RA, Miralles GD, Grp TS (2005) T-1249 retains potent antiretroviral activity in patients who had experienced virological failure while on an enfuvirtide-containing treatment regimen. J Infect Dis 191(7):1155–1163. doi:10.1086/427993

Laue TM, Shah BD, Ridgeway TM, Pelletier SL (eds) (1992) Analytical ultracentrifugation in biochemistry and polymer science, Royal Society of Chemistry, London, pp 90–125

Leman LJ, Weinberger DA, Huang ZZ, Wilcoxen KM, Ghadiri MR (2007) Functional and mechanistic analyses of biomimetic aminoacyl transfer reactions in de novo designed coiled coil peptides via rational active site engineering. J Am Chem Soc 129(10):2959–2966. doi:10.1021/ja068052x

Liu J, Deng YQ, Li QN, Dey AK, Moore JP, Lu M (2010) Role of a putative gp41 dimerization domain in human immunodeficiency virus type 1 membrane fusion. J Virol 84(1):201–209. doi:10.1128/jvi.01558-09

Lu M, Kim PS (1997) A trimeric structural subdomain of the HIV-1 transmembrane glycoprotein. J Biomol Struct Dyn 15(3):465–471

Naito T, Izumi K, Kodama E, Sakagami Y, Kajiwara K, Nishikawa H, Watanabe K, Sarafianos SG, Oishi S, Fujii N, Matsuoka M (2009) SC29EK, a peptide fusion inhibitor with enhanced alpha-helicity, inhibits replication of human immunodeficiency virus type 1 mutants resistant to enfuvirtide. Antimicrob Agents Chemother 53(3):1013–1018. doi:10.1128/aac.01211-08

Nishikawa H, Nakamura S, Kodama E, Ito S, Kajiwara K, Izumi K, Sakagami Y, Oishi S, Ohkubo T, Kobayashi Y, Otaka A, Fujii N, Matsuoka M (2009) Electrostatically constrained alpha-helical peptide inhibits replication of HIV-1 resistant to enfuvirtide. Int J Biochem Cell Biol 41(4):891–899. doi:10.1016/j.biocel.2008.08.039

Otaka A, Nakamura M, Nameki D, Kodama E, Uchiyama S, Nakamura S, Nakano H, Tamamura H, Kobayashi Y, Matsuoka M, Fujii N (2002) Remodeling of gp41-C34 peptide leads to highly effective inhibitors of the fusion of HIV-1 with target cells. Angew Chemie Int Edn 41(16):2938–2940

Qi Z, Shi WG, Xue N, Pan CG, Jing WG, Liu KL, Jiang SB (2008) Rationally designed anti-HIV peptides containing multifunctional domains as molecule probes for studying the mechanisms of action of the first and second generation HIV fusion inhibitors. J Biol Chem 283(44):30376–30384. doi:10.1074/jbc.M804672200

Schuck P (2000) Size distribution analysis of macromolecules by sedimentation velocity ultracentrifugation and Lamm equation modeling. Biophys J 78:1606–1619

Sieber SA, Marahiel MA (2005) Molecular mechanisms underlying nonribosomal peptide synthesis: approaches to new antibiotics. Chem Rev 105(2):715–738. doi:10.1021/cr0301191

Singh J, Petter RC, Baillie TA, Whitty A (2011) The resurgence of covalent drugs. Nat Rev Drug Discov 10(4):307–317. doi:10.1038/nrd3410

Tan K, J-h Liu, J-h Wang, Shen S, Lu M (1997) Atomic structure of a thermostable subdomain of HIV-1 gp41. Proc Natl Acad Sci USA 94(23):12303–12308

Weissenhorn W, Dessen A, Harrison SC, Skehel JJ, Wiley DC (1997) Atomic structure of the ectodomain from HIV-1 gp41. Nature 387(6631):426–430

Wexler-Cohen Y, Shai Y (2007) Demonstrating the C-terminal boundary of the HIV 1 fusion conformation in a dynamic ongoing fusion process and implication for fusion inhibition. FASEB J 21(13):3677–3684. doi:10.1096/fj.07-8582com

Wilcoxen KM, Leman LJ, Weinberger DA, Huang ZZ, Ghadiri MR (2007) Biomimetic catalysis of intermodular aminoacyl transfer. J Am Chem Soc 129(4):748–749. doi:10.1021/ja067124h

Wild C, Oas T, McDanal C, Bolognesi D, Matthews T (1992) A synthetic peptide inhibitor of human-immunodeficiency-virus replication—correlation between solution structure and viral inhibition. Proc Nat Acad Sci USA 89(21):10537–10541

Wild C, Dubay JW, Greenwell T, Baird T, Oas TG, McDanal C, Hunter E, Matthews T (1994) Propensity for a leucine zipper-like domain of human-immunodeficiency-virus type-1 gp41 to form oligomers correlates with a role in virus-induced fusion rather than assembly of the glycoprotein complex. Proc Nat Acad Sci USA 91(26):12676–12680

Yi HA, Diaz-Aguilar B, Bridon D, Quraishi O, Jacobs A (2011) Permanent inhibition of viral entry by covalent entrapment of HIV gp41 on the virus surface. Biochemistry 50(32):6966–6972. doi:10.1021/bi201014b

Zhou NE, Kay CM, Hodges RS (1993) Disulfide bond contribution to protein stability—positional effects of substitution in the

hydrophobic core of the 2-stranded alpha-helical coiled-coil. Biochemistry 32(12):3178–3187. doi:10.1021/bi00063a033

Zhu Y, Lu L, Xu LL, Yang HW, Jiang SB, Chen YH (2010) Identification of a gp41 core-binding molecule with homologous sequence of human TNNI3K-like protein as a novel human immunodeficiency virus type 1 entry inhibitor. J Virol 84(18):9359–9368. doi:10.1128/jvi.00644-10